

## Multi-proxy reconstructions of northeastern Pacific sea surface temperature data from trees and Pacific geoduck

Bryan A. Black<sup>a,\*</sup>, Carolyn A. Copenheaver<sup>b</sup>, David C. Frank<sup>c</sup>, Matthew J. Stuckey<sup>a</sup>, Rose E. Kormanyos<sup>a</sup>

<sup>a</sup> Hatfield Marine Science Center, 2030 SE Marine Science Drive, Oregon State University, Newport, OR 97365, USA

<sup>b</sup> Forestry Department, 228 Cheatham Hall, Virginia Tech; Blacksburg, VA 24061, USA

<sup>c</sup> Swiss Federal Institute for Forest, Snow, and Landscape Research, Dendro Sciences Unit, Zürcherstrasse 111, 8903 Birmensdorf, Switzerland

### ARTICLE INFO

#### Article history:

Received 19 December 2008

Received in revised form 4 April 2009

Accepted 6 April 2009

#### Keywords:

Dendrochronology

Sclerochronology

Sea surface temperatures

Climate change

### ABSTRACT

We demonstrate the potential for developing sea surface temperature (SST) reconstructions in the northeast Pacific from combinations of tree-ring and growth-increment chronologies of the long-lived marine bivalve, the Pacific geoduck. Six Pacific geoduck chronologies developed from site along the Washington–British Columbia coast are compared and combined with tree-ring chronologies from California to Alaska. All chronologies are annually resolved and strongly relate to local to regional-scale SST, though differences in the response season as well as the spectral properties of the two proxies are observed. Both proxy types closely track SST and when used in combination, yield a more robust SST reconstruction than tree-ring or geoduck chronologies could provide alone. In total, variance explained in SST is 63.9% at the regional-scale and 68.2% at a local scale, providing SST estimates for more than 60 years prior to the start of continuous instrumental records in this region. This study represents one of the few climate reconstructions where both proxies are annually resolved, and is the first to integrate regional networks of geoduck chronologies and tree-ring chronologies.

© 2009 Elsevier B.V. All rights reserved.

### 1. Introduction

Due to limitations in the length and distribution of instrumental climatic records, biotic and abiotic proxies have proven critical in providing context for interpreting current climate patterns and establishing historical ranges of variability. Tree-ring data are the archetypal example of such proxies, and have been widely used to reconstruct various climatic phenomena including temperature, precipitation, snowpack, ice storms, and river discharge (Prieto et al., 1999; Lafon and Speer, 2002; Woodhouse, 2003; Briffa et al., 2004). Data are annually resolved, often span several hundred years, and can be extended over millennia when chronologies from living trees are combined with dead wood samples (Kadonaga et al., 1999; Cook et al., 2004; D'Arrigo et al., 2005a; Wilson et al., 2005; Buntgen et al., 2006). Trees can also serve as proxies for broad-scale patterns of ocean-atmosphere circulation such as the Pacific Decadal Oscillation, the El Niño Southern Oscillation, or the North Atlantic Oscillation (Cook et al., 2002; MacDonald and Case, 2005). However, tree-ring based reconstructions of the marine environment are limited to those processes that are closely coupled with the atmosphere and transferred over land. In addition, the vast majority of tree-ring records are limited to temperate regions where a regular dormancy period ensures annual ring formation, though advances have been made in

developing chronologies from tropical species (Cook et al., 2002; Baker et al., 2008; Chowdhury et al., 2008). These spatial constraints are further limited by the dependence of tree-response upon climatology, site, and species, with, for example, skillful temperature sensitive sites confined to altitudinal or latitudinal tree-line locations (Esper et al., 2002; D'Arrigo et al., 2006a).

Analogous to trees, a number of animal species form annual growth increments, and these organisms have been increasingly used to assess climate variability in marine systems. The majority of these studies involve bivalves or hermatypic corals, though otoliths and coralline algae have also proven useful (Strom et al., 2004; Goodkin et al., 2005; Halfar et al., 2007; Thresher et al., 2007). Chemical or isotopic signatures such as <sup>18</sup>O or Sr/Ca ratios are most often utilized as environmental proxies, and morphological attributes including growth-increment width or luminance profiles are also effective (Hendy et al., 2003; Schöne et al., 2004). Reconstructions can encompass several hundred years and provide data across a wide range of depths, latitudes, and life histories (Hendy et al., 2003; Schöne et al., 2003).

A relatively recent advance in these marine chronologies is the application of the tree-ring technique of crossdating to ensure that all growth increments are assigned the correct calendar year. The technique involves matching among all the numerous specimens from a site the synchronous ring-width patterns induced by climate (Stokes and Smiley, 1996). Should an increment be absent or misidentified in an individual, the growth pattern will be offset relative to that

\* Corresponding author. Fax: +1 541 867 0137.

E-mail address: [bryan.black@oregonstate.edu](mailto:bryan.black@oregonstate.edu) (B.A. Black).

in the other samples, helping to identify the dating error. Crossdating has been successfully applied to develop annually resolved growth-increment chronologies in corals, marine and freshwater bivalves, and Pacific rockfish otoliths (Hendy et al., 2003; Helama et al., 2006b; Black et al., 2008b). Final chronologies are of a quality comparable to tree-ring data, relate strongly to climatic indices, and can be used to generate high-resolution climate reconstructions. So far crossdated tree-ring, bivalve, and fish (otolith or scale) chronologies have been used to investigate interrelationships among marine, freshwater, and terrestrial habitats, thereby showing linkages across diverse species and ecosystems (Guyette and Rabeni, 1995; LeBreton and Beamish, 2000; Schöne et al., 2004).

A particularly attractive feature of multiple and diverse environmental proxies is that they can be used to reinforce and corroborate one another. Each archive records climate variability from its unique “perspective” of habitat, location, life history, or trophic level such that their combination yields a more holistic perspective of the past than any data set could provide on its own. For example, tree-rings, corals, boreholes, and ice cores all contribute to demonstrate a common trend of increasing global temperature over the past 150 years (IPCC, 2007), with different proxy types contributing more skillfully to a particular spatial or seasonal domain (Pauling et al., 2003). Likewise, networks of coral and tree-ring chronologies offer new insight into the historical dynamics of the Pacific Decadal Oscillation and El Niño Southern Oscillation over the past several centuries (Gedalof et al., 2002; D’Arrigo et al., 2005b). Despite these promising results, the benefits of combining crossdated tree-ring and sclerochronologies (from hard parts of animals) in multi-proxy climate reconstructions remains poorly explored.

In this study, we develop sea surface temperature (SST) reconstructions in the northeast Pacific from combinations of tree-ring and Pacific geoduck growth-increment chronologies. Pacific geoduck is a

long-lived nearshore bivalve that can be crossdated and can hence be used to generate annually resolved growth chronologies. Additionally, geoduck chronologies strongly relate to environmental variability, and have been utilized to reconstruct SST in regions of the North Pacific (Strom et al., 2004). A large number of tree-ring chronologies have also been developed throughout Alaska and the Pacific Northwest, and independently used to reconstruct SST, as well as other aspects of ocean circulation. Thus, the objectives of this study are to describe the properties of geoduck and tree-ring chronologies and evaluate the degree to which a combination of these data types increased the degree of skill in reconstructing SST. In so doing, this provides one of the few attempts to reconstruct climate variability from two annually resolved climate proxies.

## 2. Data and methods

Pacific geoduck (*P. abrupta*) range from Kodiak, Alaska to southern California and can be found buried in ocean floor sediment from the lower intertidal to depths up to 100 m (Bernard, 1983; Coan et al., 2000). For five of the chronologies, geoducks were live-collected along the British Columbia coast in 2003 and 2004 by the Department of Fisheries and Oceans Canada (DFO) Pacific Biological Station in Nanaimo, BC (Fig. 1). To prepare growth increments for analysis, a single shell from each geoduck specimen was cut along the height axis of the valve through the center of the hinge plate region using a diamond-blade lapidary saw. The cut surface was polished with 600-grit sandpaper and then etched with two-percent hydrochloric acid. An impression (acetate peel) was made by pressing the etched surface of the hinge plate region against a piece of acetate film softened with a drop of acetone. The resulting peel was placed between two glass slides and viewed through a dissecting microscope using transmitted light. The hinge plate (inner shell layer) grows at a rate proportional to

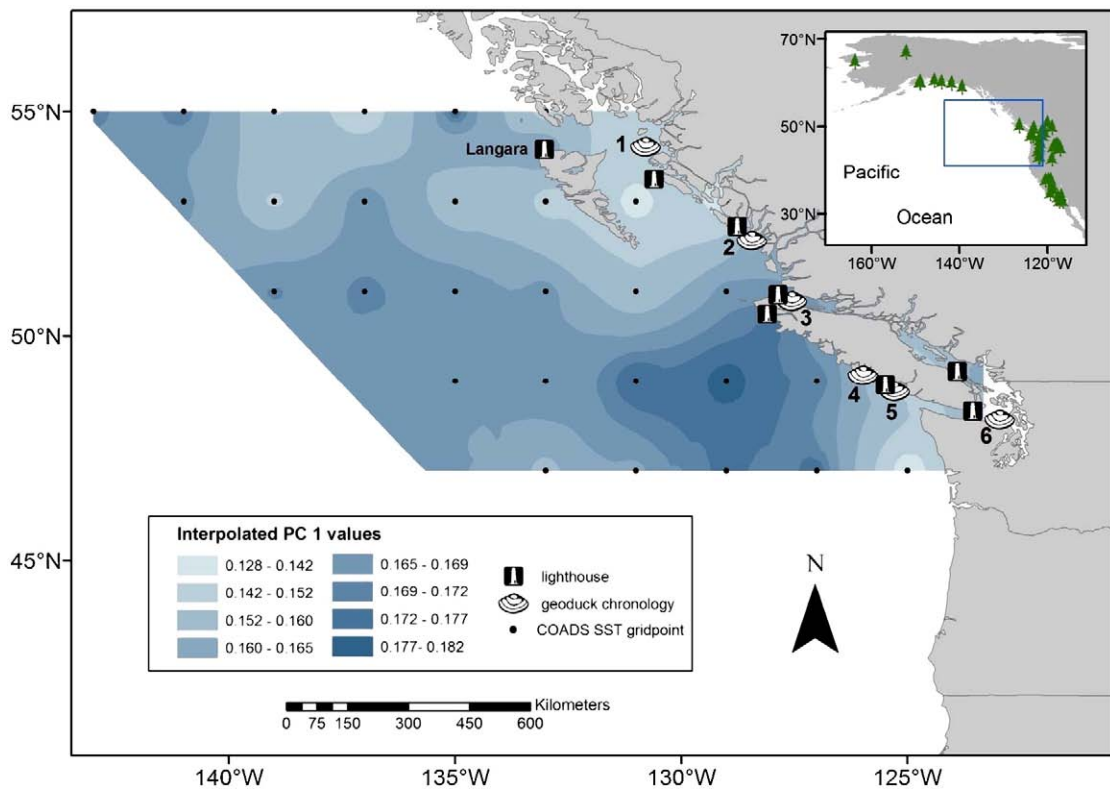


**Fig. 1.** Map of the study region with locations of geoduck chronologies and sea surface temperature (SST) data sources including lighthouse stations and COADS grid points. Also shown is the first principal component extracted from all SST data (1961:2005). Inset map indicates locations of tree-ring chronologies that significantly ( $p < 0.01$ ) correlated with SST data from Langara lighthouse or the first principal component of all SST data. Geoduck chronologies are 1) Tree Nob, 2) Cape Mark, 3) Goletas, 4) Bartlett, 5) Brady's Beach, and 6) Strom.

that of the outer shell layer, but is better protected from erosion and provides the most complete record possible. All peel preparation was conducted by the DFO.

Individuals, selected on the basis of age and the clarity of annual bands, were visually crossdated within each site using the list-year technique (Yamaguchi, 1991). Then, under the dissecting microscope at 60× magnification, two to eight overlapping digital photographs were taken with a Leica DC300 7.2 megapixel camera and tiled into a single panoramic image using Image Pro Plus 6.0 (Media Cybernetics Inc., Silver Spring, MD). In Image Pro Plus 6.0, growth-increment widths were measured along continuous transects that followed the axis of growth. Each growth-increment was delineated at the end of the winter line (start of the new growing season). Crossdating at each site was validated using the International Tree-Ring Data Bank Dendrochronology Program Library (ITRDB DPL) program COFECHA. As part of crossdating verification, COFECHA detrended each measurement time series with a cubic spline set at a 50% frequency response of 22 years (Holmes, 1983; Grissino-Mayer, 2001; Black, 2009). Each detrended measurement time series was then correlated with the average of all other detrended measurement time series, and the mean for each site was reported as the series intercorrelation.

To develop a master chronology at each site, measurement time series were detrended using negative exponential functions in program ARSTAN developed by Ed Cook and Paul Krusic, available at [<http://www.ldeo.columbia.edu/res/fac/trl/public/publicSoftware.html>] (Cook, 1985). Once completed, the quality of the chronology was quantified using the Expressed Population Signal (EPS) statistic, which describes how well the sample means represents the mean of the theoretical population from which it was drawn. Though there is no significant threshold for this statistic, an EPS value of 0.85 or greater is considered adequate (Wigley et al., 1984). The mean sensitivity, an index of the strength of high-frequency, year-to-year variability was also calculated (Fritts, 1976). The sixth chronology was developed by Strom et al. (2004) using similar techniques and was obtained from the NOAA Paleoclimate Database [<http://www.ncdc.noaa.gov/paleo/paleocean.html>] (Fig. 1). Crossdating and EPS were verified using the original growth-increment measurements.

Sea surface temperature (SST) data were obtained from eight lighthouse stations along the British Columbia coast (SST<sub>LH</sub>; [http://www.pac.dfo-mpo.gc.ca/sci/osap/data/Search\\_Tools/Searchlighthouse\\_e.htm](http://www.pac.dfo-mpo.gc.ca/sci/osap/data/Search_Tools/Searchlighthouse_e.htm)) as well as 2° × 2° gridded SST data available through the International Comprehensive Ocean-Atmosphere Data Set (ICOADS) (SST<sub>ICOADS</sub>; <http://icoads.noaa.gov/index.shtml>) (Fig. 1). Patterns in SST<sub>ICOADS</sub> data were explored using principal components analysis (PCA) on the 1961–2005 common interval. These dates provided the best balance between time series length and the completeness of the records, considering that the rate of missing observations increased dramatically prior to 1961. All SST data were provided as monthly averages. In some time series, however, a maximum of two monthly values were missing, but these could be filled using regressions of temperature data from previous months or adjacent locations (generally an  $R^2$  of approximately 0.7). Once all monthly data were complete over this 45 year period, mean annual sea surface temperatures were calculated and entered into PCA. The first principal component (1961–2005) captured 72.2% of the variance in the data set. Eigenvalues for all gridpoints were positive and ranged from 0.128 to 0.182 while factor loadings ranged from 0.67 to 0.97 (mean = 0.85), indicating a strong common signal (Fig. 1). Eigenvalues experienced the greatest gradients from the north to south along the British Columbia coastline (Fig. 1). The second and third principal components explained only an additional 6.2% and 5.0%, respectively, and were therefore removed from further analysis. Six of the lighthouse stations spanned 1942 through 2005. When principal components analysis was performed on this subset, the first component (SST PC1) captured 86.1% of the variance. In a regression between the first principal component for the full data set and that from the six light houses, the  $R^2$  was 0.91, indicating strong agreement. Thus, we retained the principal

component from the longer SST records (SST PC1) to maximize the length of the regional SST time series and the overlap with geoduck and tree-ring chronologies.

Reconstructions were performed for the first principal component of the regional SST data (SST PC1), and also for SST records at Langara Lighthouse, located in the northern portion of the study area (Fig. 1). This station, situated at the northern tip of the Queen Charlotte Islands, was highly exposed to the open Pacific Ocean, correlated particularly well with tree-ring and geoduck chronologies, and as such was a strong candidate for a reconstruction. Dependent variables included geoduck chronologies as well as tree-ring chronologies from Alaska, British Columbia, Washington, Oregon, and California obtained from the NOAA Paleoclimate International Tree Ring Data Bank (ITRDB) website [<http://www.ncdc.noaa.gov/paleo/treering.html>]. Only those data sets that extended through 1990 or later (i.e. sites sampled after 1990) were retained to maximize overlap with sea surface temperature data. The standard chronology was downloaded where available; otherwise a standard chronology was generated from the original ring with data using negative exponential detrending.

A total of two reconstruction methods were attempted for the regional SST data (SST PC1) and also for Langara Lighthouse, each using chronologies that significantly and positively correlated ( $p < 0.01$ ) with the given SST data set. In the first approach, all tree-ring chronologies were averaged into a composite chronology, and the geoduck chronologies were averaged into a second composite chronology. The composite (average) tree-ring and geoduck chronologies were then related to SST records via stepwise linear regression with a  $p < 0.01$  threshold to enter. In the second approach, principal components regression was applied using the original (individual) tree-ring and geoduck chronologies. Principal components were selected for the model using the same stepwise procedure. In all models, predictor variables were lagged by  $t + 1$  and  $t - 1$  to account for the possibility that the previous year's climate could affect the current year's growth (Fritts, 1976). To validate the reconstructions, Mallow's  $C_p$  and variance inflation factors were calculated followed by a bootstrapping analysis. In the first step of bootstrapping, a calibration data set equal to the number of years common to the geoduck chronologies and the SST data was randomly selected with replacement. Thus, some years were omitted while other years were selected multiple times, and those years not selected were used as an independent verification data set. For the dependent and independent data sets, the mean and standard deviation of model parameters were calculated as were  $R^2$  and the reduction of error coefficient (RE) (Fritts, 1976). A total of 500 iterations were conducted. The RE is a measure of shared variance between the independent data and the values modeled from the calibration data set. The maximum theoretical value of the RE statistic is +1 and any positive value indicates that the regression model has some degree of skill (Fritts, 1976).

### 3. Results

Mean sensitivity values exceeding 0.2 and series intercorrelations exceeding 0.67 indicated that growth varied considerably from year to year, and that these growth patterns were highly synchronous within sites (Table 1). Such strongly conserved growth patterns were also apparent in the raw and detrended measurement time series (Fig. 2A,B). EPS consistently exceeded values of 0.85 once sample depth reached six to eight measurement time series, and final chronologies spanned 55–123 years in length after truncation at the  $EPS > 0.85$  threshold (Table 1).

Although geoduck chronologies generally tracked one another as well as the first principal component from the regional SST data (SSTPC1), correlations between individual geoduck chronologies and the SSTPC1 were variable, ranging from 0.27 to 0.63 (Table 1; Fig. 2C,D). The site with the lowest correlations, Brady's Beach, was

**Table 1**  
Chronology summary statistics arc correlations with sea surface temperature data.

	Measured series (n) <sup>a</sup>	Mean sensitivity <sup>b</sup>	Series inter correlation <sup>c</sup>	Span <sup>d</sup>	SST PC1 correlation <sup>e</sup>
Tree Nob	66	0.29	0.74	1888:2003	0.56***
Cape Mark	28	0.25	0.67	1907:2003	0.27*
Goletas	22	0.23	0.76	1948:2002	0.45***
Bartlet	40	0.24	0.71	1937:2003	0.36**
Brady's Beach	27	0.22	0.71	1934:2001	0.21
Strom	74	0.25	0.76	1877:1999	0.62***

<sup>a</sup> The number of measurement time series used in developing each chronology.  
<sup>b</sup> An index of high-frequency variability.  
<sup>c</sup> The average correlation between each detrended time series (using a 22-year cubic spline) and the average of all other detrended measurement time series, as output by COFECHA.  
<sup>d</sup> Chronology length at which expressed population signal (EPS) > 0.85.  
<sup>e</sup> Correlation coefficient between each chronology and the first principal component of sea surface temperature data (SST PC1) from the region; significance: \*\*\* $p < 0.001$ ; \*\* $p < 0.01$ ; \* $p < 0.05$ .

not significant at the  $p < 0.05$  level, a threshold barely exceeded by Cape Mark (Table 1). When compared to SST data from individual lighthouses or other indicators of ocean variability such as upwelling, the Northern Oscillation Index, or Pacific Decadal Oscillation, correla-

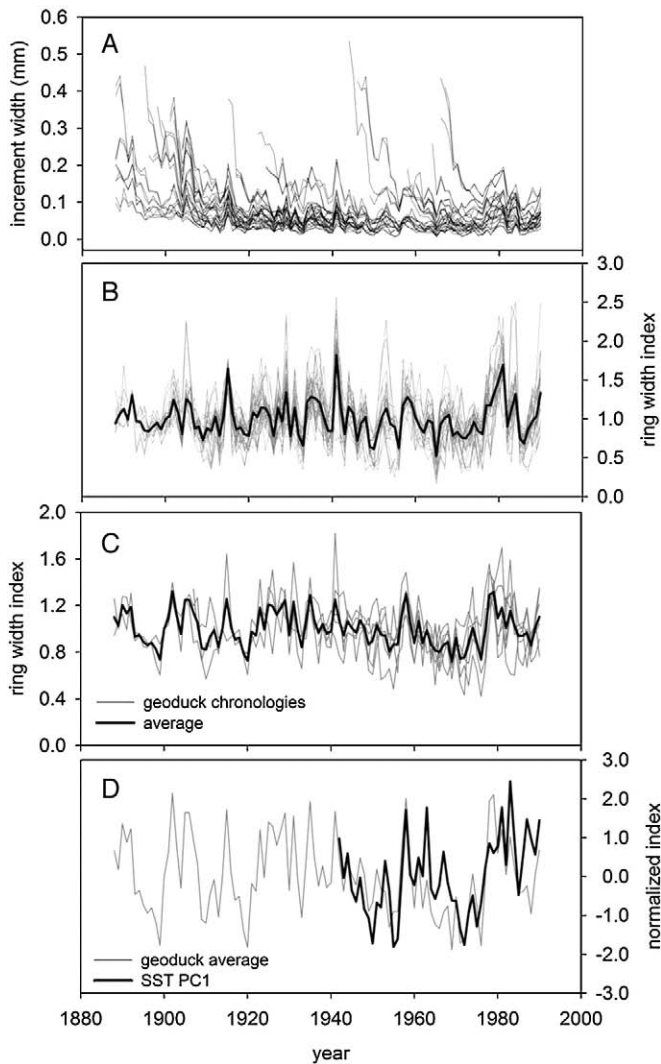


**Fig. 2.** A) Measurement time series for geoduck in the Tree Nob chronology. B) Tree Nob master chronology (heavy line) and individual measurement time series after detrending with negative exponential functions. C) The six master geoduck chronologies and their average. D) The average of the six geoduck chronologies and the leading principal component for regional SST (SST PC1).

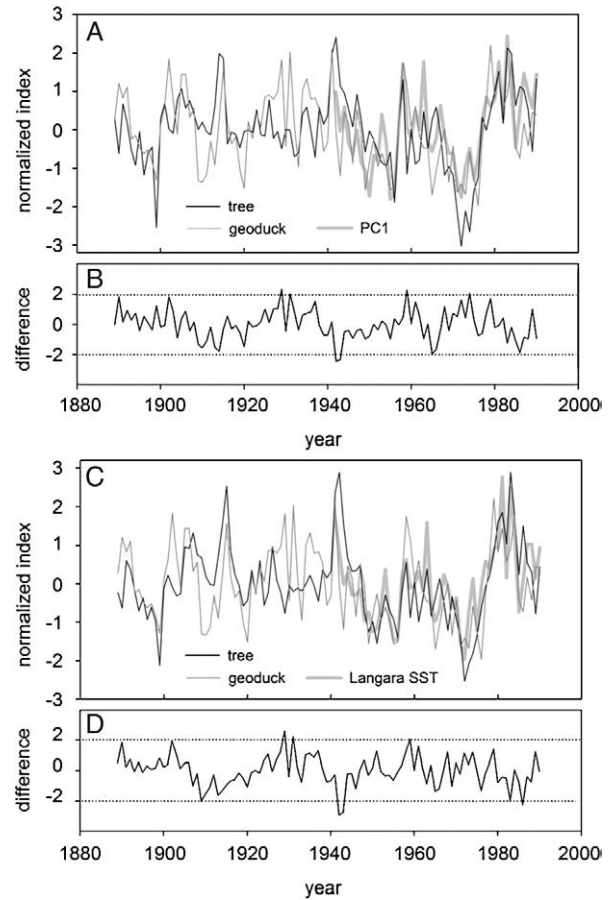


**Fig. 3.** The composite (average) of all tree-ring chronologies significantly related to SST, the composite (average) or the Tree Nob and Strom chronologies, and the SST instrumental record for A) the leading principal component of SST for the British Columbia coastal region, and C) Langara Lighthouse. All data are normalized to a mean of zero and a standard deviation of one. B) and D) show the difference between the tree-ring and geoduck composite chronologies.

tion coefficients remained low (data not shown). By contrast, correlations between the SSTPC1 and the Tree Nob, Strom, and Goletas chronologies were much stronger (Table 1).

For SST reconstructions, only the Tree Nob and Strom geoduck chronologies were included due to their much greater lengths. Both were highly significantly ( $p < 0.01$ ) correlated to SST PC1 as well as SST data from Langara Lighthouse. Among the 240 tree-ring chronologies, a total of 55 were significantly ( $p < 0.01$ ) correlated to SST PC1 while 34 significantly correlated with SST data from Langara Lighthouse. Twenty-nine of these 34 chronologies were significant for both Langara and SST PC1. Though tree-ring chronologies ranged from California to Alaska (Fig. 1), correlations with SST data were always positive. The average of all significant ( $p < 0.01$ ) tree-ring chronologies (the composite chronology) and the average of the Tree Nob and Strom et al. (2004) chronologies tracked one another as well as the regional SST record (SST PC1) (Fig. 3A) and the Langara Lighthouse SST record (Fig. 3C). Indeed, differences between the two composite chronologies rarely exceeded two standard deviations (Fig. 2B and D).

Peak correlations between monthly-resolved SST from Langara Lighthouse and i) the composite tree-ring chronology and ii) the composite geoduck chronology used in the Langara reconstruction indicated that each species has a slightly different climate sensitivity (Fig. 4). Though correlations with annual SST were comparable, the composite tree-ring chronology was more strongly related to SST in the winter and spring while the composite geoduck chronology was more sensitive to the summer months (Fig. 4). The spectral properties of each proxy also differed according to a wavelet analysis. The tree

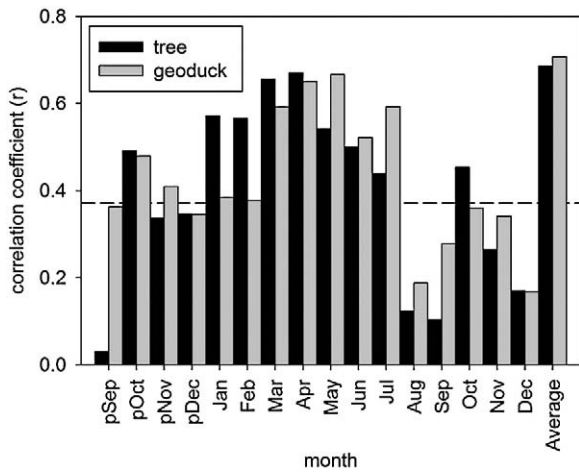


**Fig. 4.** Correlation between monthly averaged SST data from Langara Lighthouse Station and i) the composite (average) tree-ring chronology and ii) the composite (average) geoduck chronology used in the Langara Lighthouse SST reconstructions. A 16-month period is shown, including 4 months prior (p) to the current calendar year. Dotted line indicates significance at the  $p < 0.01$  level.

composite chronology contained significant oscillations at periods ranging from 2 to 8 years, as well as those between 16 and 32 years (Fig. 5A). By contrast, the periods with the most power in the geoduck chronology generally ranged from 8 to 16 years, though there were also some significant oscillations from 2 to 4 years (Fig. 5B).

In a comparison between a SST reconstruction via principal components regression (PCR) and reconstruction via a multiple regression using the composite geoduck chronology and the composite tree-ring chronology, the multiple regression using the composite chronologies (the composite models) provided greater  $R^2$  values than

PCR. For both SST PC1 and Langara Lighthouse,  $R^2$  in the composite model exceeded that in the PCR on average by 0.13. Furthermore, in the composite models  $C_p$  values were low and variance inflation factors for both variables were 1.50, indicating that collinearity was not destabilizing the model (Table 2B,C). In bootstrapping analysis of the composite chronology models, parameters in the dependent and independent data sets closely agreed with one another for both the SST PC1 and Langara Lighthouse reconstructions (Table 2B,C). Ninety-five percent confidence intervals were relatively narrow and overlapped between dependent and independent parameter estimates, with the one exception of the Langara Lighthouse geoduck slope in which the independent estimate was slightly greater than the dependent estimate (Table 2C). As an additional indicator of reconstruction skill, the reduction of error statistic was strongly positive for both models (Table 2B,C).

In combination, Pacific geoduck and tree-ring data provided more robust SST reconstructions than either data type could provide alone. For example, the composite Tree Nob and Strom geoduck chronology accounted for 49.9% of the variance of SST PC1 while the tree-ring composite chronology alone accounted for 49.4% of the variance. Principal components regression on these 55 tree-ring chronologies yielded a similar result with 48.6% of the variance explained, using a stepwise ( $p < 0.01$  threshold to enter) model. Thus, geoduck and tree-ring data together provided a clear improvement in the SST

**Table 2**

Summary statistics for sea surface temperature (SST) reconstructions derived from tree-ring and Pacific geoduck data. A) comparison of two reconstruction techniques: a “composite” technique in which all tree-ring chronologies that were significantly correlated to SST data were averaged into a single composite chronology, as were the two longest geoduck chronologies. Then the two composite chronologies (geoduck and tree-ring) were related to SST data via a two-variable multiple regression. The same chronologies were also entered into principal components regression (PCR). Two SST data sets were tested: the first principal component of all SST data in the region (SST PC1) as well as SST records from Langara Lighthouse. B) Parameter estimates and  $R^2$  values for the composite chronology reconstruction of SST PC1 are shown for the full data set (1942–1990) as well as those calculated for dependent and independent data sets in a bootstrapping analysis, including 95% confidence intervals and the reduction of error statistic. C) Parameter estimates and bootstrapping analysis for Langara Lighthouse (1941–1990).

**A. Comparison of principal components regression (PCR) and composite chronology results**

Model	Composite chronologies		PCR	
	SST PC1	Langara	SST PC1	Langara
$R^2$	63.90	68.23	50.87	55.6
Mallow's $C_p$	3.00	3.00	22.16	15.23
Significance	$p < 0.0001$	$p < 0.0001$	$p < 0.0001$	$p < 0.0001$
Dependent variables	2	2	2	1

**B. SST PC1 reconstruction: composite chronologies**

	All data	Bootstrap: calibration data		Bootstrap: independent data	
		Mean	95% CI	Mean	95% CI
$R^2$	63.90	64.80	±0.64	65.30	±0.91
Intercept	-12.98	-13.04	±0.12	-13.11	±0.17
Tree slope	7.80	7.74	±0.14	7.92	±0.20
Geoduck slope	4.94	5.07	±0.09	4.96	±0.13
Reduction of error	Mean	95% CI			
	0.69	±0.009			

**C. Langara Lighthouse reconstruction: composite chronologies**

	All data	Bootstrap: calibration data		Bootstrap: independent data	
		Mean	95% CI	Mean	95% CI
$R^2$	68.23	68.30	±0.62	69.59	±0.92
Intercept	6.06	6.07	±0.03	6.01	±0.04
Tree slope	1.75	1.76	±0.03	1.75	±0.04
Geoduck slope	0.99	0.97	±0.02	1.04	±0.03
Reduction of error	Mean	95% CI			
	0.72	±0.009			

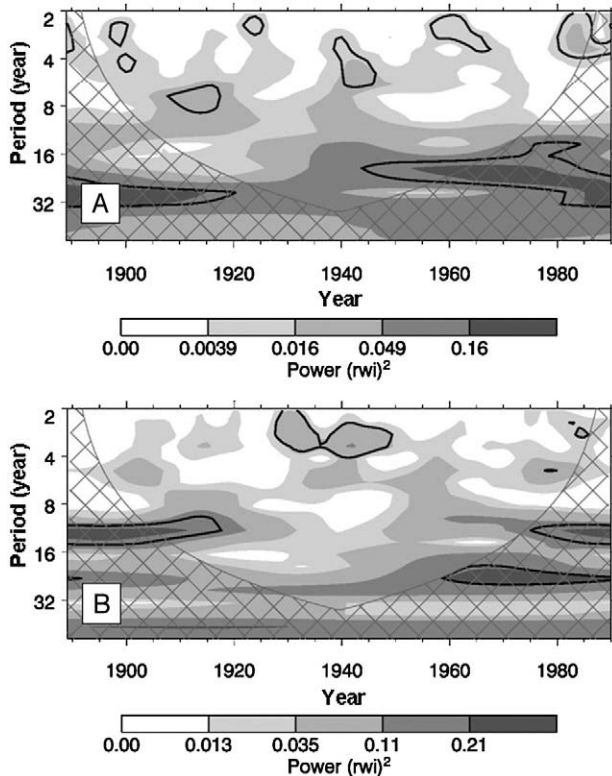


**Fig. 5.** Wavelet analysis of A) the composite (average) tree-ring chronology and B) the composite (average) geoduck chronology used in the Langara Lighthouse SST reconstruction. Black contours denote regions of significance ( $p < 0.10$ ). The cone of influence where edge effects may be important is indicated by crosshatching.

reconstruction, bringing the total variance explained to 63.9%. Such an improvement was particularly remarkable considering that it could be accomplished with only two geoduck chronologies. To better illustrate this point, we applied a sensitivity test in which one tree-ring chronology was removed from the data set ( $N = 55$  chronologies), the remaining 54 tree-ring chronologies were averaged, and the single chronology and the average chronology were entered into a two-variable multiple regression against SST PC1. When repeated for each of the 55 chronologies, the average contribution of a single tree-ring chronology was  $1.4\% \pm 0.4\%$  (mean  $\pm$  95% CI) of the total variance. This was in comparison to an additional 3.94% of variance explained when the Strom geoduck chronology was included with the composite tree-ring chronology, or the 13.9% added by the Tree Nob chronology, or the 14.5% variance added by the average of the Strom and Tree Nob geoduck chronologies.

Reconstructions closely tracked instrumental records and extended each set used in this study by more than 60 years (Fig. 6A,B). In comparison to the instrumental record, the reconstructed portion of the SST record was less variable, particularly with respect to the low-frequency domain (Fig. 6A,B). It is possible that this pattern is an artifact of methodological biases (Esper et al., 2005), but does suggest a period of reduced variability during the later 19th and early 20th centuries. In the more recent era, temperatures began a steady decline in the mid 1940s, peaking again in the mid 1960s, and declining through the 1970s after which they attained their highest values of the record (Fig. 6A,B).

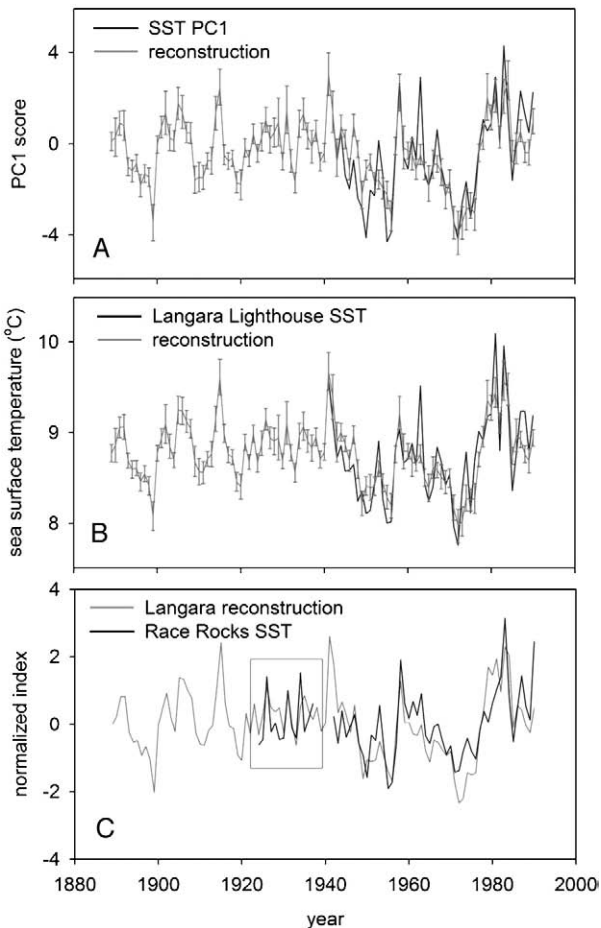


**Fig. 6.** Instrumental records and reconstructions of A) the first principal component of all sea surface temperature data for the region and B) sea surface temperature data at Langara Lighthouse. Error bars are 95% confidence intervals. C) The Langara Lighthouse SST reconstruction and SST records for Race Rocks, the southernmost lighthouse station. Inset highlights the period 1920–1940.

The Race Rocks Lighthouse SST data extended back to 1922 and provided an extra validation of the reconstructions prior to the calibration period. For the Langara reconstruction, correlation with Race Rocks annual SST after 1940 was  $r = 0.76$  ( $p < 0.01$ ;  $n = 49$ ) and before 1940 was slightly lower at  $r = 0.58$  ( $p < 0.03$ ;  $n = 17$ ). For the SST PC1 reconstruction, the post-1940 correlation with Race Rocks was  $r = 0.75$  ( $p < 0.01$ ;  $n = 49$ ) and before 1940 was  $r = 0.49$  ( $p < 0.05$ ;  $n = 17$ ). Between 1920 and 1940 was a time of particularly strong disagreement between the two proxies (Fig. 3A,C), characterized by strong oscillations in the geoduck that were unmatched by the trees. Individually, neither the tree composite chronology ( $r = 0.34$ ) nor the geoduck composite chronology ( $r = 0.41$ ) significantly ( $p < 0.05$ ) correlated with Race Rocks SST during this period. Yet in combination, the two proxies provided a much better match to the SST record (Fig. 5C), demonstrating the advantages of a multi-proxy approach.

#### 4. Discussion

Within each site Pacific geoduck exhibited strongly synchronous growth patterns, allowing for crossdating and the development of annually resolved, environmentally sensitive chronologies. Positive correlations with SST in this study were consistent with experiments in other marine bivalve species, which indicate that water temperature maintains positive control on shell growth rate, even when food is withheld and specimens lose tissue weight (Cerrato, 2000). With respect to geoduck, 1 year-old individuals maintained at a combination of elevated temperatures and high food densities experienced greater shell growth than those for which temperature or food were limited (Strom, 2003). In the field, Noakes and Campbell (1992) identified a positive relationship between geoduck growth-increment width and water temperature along the eastern side of Vancouver Island, BC. Also, the highest growth rates in the Strom et al. (2004) geoduck chronology occurred during a period with the warmest SST on record, concurrent with what were likely below-average levels of productivity. In this study, such strongly positive relationships with SST allowed the reconstruction of approximately 50% of the variance in SST records at local and regional scales. This level of skill was comparable to that found by Strom et al. (2004) at Race Rocks Lighthouse Station in Puget Sound, underscoring the potential for geoduck to nearly double the length of existing SST time series along the northeast Pacific coast (Strom et al., 2004).

Notable exceptions to these expected climate-growth relationships included Cape Mark and Brady's Beach chronologies, which did not correlate as strongly with regional SST data, SST records from the closest lighthouse station, the Pacific Decadal Oscillation, or even indices of the El Niño Southern Oscillation. Weak correlations with existing SST records may reflect the heterogeneity of the nearshore environment. Cape Mark and Brady's Beach may represent sites at least partially isolated from regional climate signals due to bathymetry, degree of mixing, or freshwater input, and existing instrumental records were unable to capture these microsite conditions.

Through broad-scale couplings between ocean and atmosphere, tree-ring chronologies were strongly linked to SST, as has been reported throughout the Pacific Northwest and Alaska (Wiles et al., 1998; D'Arrigo et al., 1999; MacDonald and Case, 2005). Even though many of the tree-ring chronologies were not necessary sampled for climate sensitivity, we found that almost a quarter of all tree-ring chronologies significantly ( $p < 0.01$ ) related to regional SST, a percentage much lower than the two-thirds of geoduck chronologies that correlated at this level, but also more than 20 times the number expected by chance alone. Furthermore, chronologies that significantly related to SST fell along a transect of elevation and latitude, ascending from sea level at approximately  $70^\circ$  latitude to 2500 m at  $35^\circ$  latitude, and described by the equation  $y = -64.622x + 44.74$  where  $x$  equals latitude in decimal degrees and  $y$  equals elevation in meters ( $R^2 = 0.70$ ;  $p < 0.001$ ). This latitudinal/altitudinal gradient

reflects sites near the thermal limits for tree survival, where growth is known to be the best indicator for temperature variability (Fritts, 1976).

The mechanisms by which ocean variability limited tree growth likely varied across the landscape. At the northern sites, warm SST values are generally associated with a warm spring and summer, which increases the growing season (Wiles et al., 1998; D'Arrigo et al., 1999; Gedalof and Smith, 2001). In the Cascade Mountains and northern Sierra Nevada, snowpack becomes an additional limiting factor, the depth of which is negatively related to SST (Wiles et al., 1998; D'Arrigo et al., 1999; Gedalof and Smith, 2001; Peterson et al., 2002). Farther south in California tree growth is most negatively impacted by drought, and at these sites precipitation is positively associated with warm SST (Biondi et al., 1999; Biondi et al., 2001). All these potential pathways should lead to positive relationships between SST and tree growth, as observed for all significant correlations in this study.

These consistently positive correlations provided the somewhat unique opportunity to average tree-ring chronologies into a composite chronology for use in SST reconstructions. However, the study area spans a very large region encompassing several climatic zones, which calls into question whether chronologies can simply be averaged. Principal components regression should better accommodate such a diverse data set by identifying important subsets and extracting their dominant growth patterns for use in the reconstruction. Yet the leading principal component for the tree-ring chronologies used in the regional SST reconstruction accounted for 23% of the variance and also closely tracked the average of the tree-ring chronologies ( $R^2 = 0.884$ ;  $p < 0.0001$ ;  $n = 102$  years). Results were nearly identical for tree-ring chronologies that were used in the Langara SST reconstruction whereby the average also mirrored the leading principal component ( $R^2 = 0.881$ ;  $p < 0.0001$ ;  $n = 102$  years). Thus, in this case the composite (average) tree-ring chronologies captured a very similar pattern from the tree-ring data as the leading principal component, yet provided a less distilled model that accounted for a greater amount of variance in the SST instrumental records.

The advantage of using both geoduck and tree-ring data was that both proxies corroborated one another to provide independent verification of SST trends, yet also contributed somewhat differing aspects of the climate signal. Although the geoduck and tree-ring composite chronologies generally and consistently followed one another, only a quarter of the total variance was shared between them ( $R^2 = 0.23$  for geoduck and trees in the Langara reconstruction;  $R^2 = 0.25$  for geoduck and trees in the SST PC1 reconstruction). Such differences were reflected by the unique spectral properties and climate-growth relationships exhibited by each species, in large part due to their contrasting life histories, habitats, and mechanisms through which climate was integrated into growth-increment width. While considerable overlap in the climatic response of the two proxy archives exists, the tree-rings contributed unique information for January–February and the geoducks had strongest signals from May–July, resulting in strong relationships with annual SST. With respect to spectral properties, some dissimilarities between geoduck and tree-ring data may be an artifact of longevity and chronology development. More specifically, the process of detrending removes not only age- or geometrically-related growth declines, but also any signals at wavelengths longer than the measurement time series (Cook et al., 1995). Given that the length of measurement time series for geoduck was on the order of decades while that for most trees was on the order of centuries, the tree-ring chronologies would be more prone to capture low-frequency variability. Signals between 16 and 32 years in periodicity were indeed more pronounced in the tree-ring composite chronologies.

Overall, this combination of geoduck and tree “perspectives” clearly improved the skill of the SST reconstructions, as reflected by

the high  $R^2$  values and strength of verification measures, even during the period between 1920 and 1940 when geoduck and tree series showed the greatest differences. The final reconstructions are also corroborated by broad-scale patterns in ocean variability that have been previously documented, such as the switch in the North Pacific to a cool regime around 1945, followed by a shift to a warm regime beginning in 1977 (Mantua et al., 1997). More work is needed to understand the biological and climatic processes that contribute to the differences between proxies. Yet the results indicate that both trees and geoduck are both strong and complementary SST proxies. Other reconstruction “targets” (i.e. months or seasons) could also be considered for future work, but given ease of interpretation and strength of relationships between proxies and the instrumental records, we chose annual SST for this study.

To date, several studies have used multiple climate proxies from the same record such as chemical, isotopic, or morphological attributes from growth-increment data, or biotic and abiotic constituents of sedimentary records. Yet few have utilized proxies from entirely different sources despite their power to investigate inter-relationships among diverse taxa and ecosystems (Guyette and Rabeni, 1995; LeBreton and Beamish, 2000; Black, 2009), corroborate climate trends, especially across broad spatial scales (Mann et al., 1998; D'Arrigo et al., 2005b; Moberg et al., 2005), and to develop multi-proxy climate reconstructions (Gedalof et al., 2002; Solomina et al., 2005; Yang et al., 2007). Aspects of climate addressed by these multi-proxy studies include precipitation and drought, temperature at hemispheric and global scales, dust storm frequency, and broad-scale ocean and atmospheric variability from tree-rings, corals, speleothems, ice cores, and varves (Gedalof et al., 2002; Solomina et al., 2005; D'Arrigo et al., 2006b; Yang et al., 2007; Tompkins et al., 2008).

A challenge in many of these reconstructions is that some proxies are not annually resolved. Though they contain highly valuable information on longer-term trends, the high-frequency component of a reconstruction is lost under such circumstances and there are few degrees of freedom to robustly calibrate and verify the low-frequency component. In this study, geoduck and tree-ring data underscore the potential for using multiple annually resolved proxies in climate reconstructions. One of the shortcomings is that the geoduck chronologies are relatively short in length, typically 120 year or less. However, given uncertainties even during the mid 20th century for SST data (Thompson et al., 2008), even short chronologies may provide a valuable role in assessing climate change. Furthermore, if the growth patterns from dead geoduck individuals recovered from ocean sediments could be appended to living chronologies, as has been done with tree-rings from archeological timbers and preserved wood samples (Bortolot et al., 2001; Wilson et al., 2004), multi-centennial length reconstructions may also be achievable. Overall, geoduck represent a valuable data source for climate reconstructions in the marine environment, either in combination with other proxies or alone. As more annually resolved sclerochronologies are constructed in other regions (Helama et al., 2006a; Helama et al., 2007; Black et al., 2008a), the possibilities and value of multi-proxy reconstructions will undoubtedly continue to expand.

## Acknowledgements

The work for this project was completed with funding from the NSF Research Experience for Undergraduates program at the Hatfield Marine Science Center, a grant provided by the Department and Fisheries and Oceans (DFO), Canada, and a research sabbatical provided to CAC by Virginia Tech. DCF acknowledges support from the Swiss National Science Foundation (NCCR-Climatic). Special thanks also to the DFO for preparing and generously providing samples, as well as to the Sclerochronology Group of the 16th Annual North American Dendroecology Fieldweek, which helped develop the Tree Nob geoduck chronology.

## References

- Baker, P.J., Palmer, J.G., D'Arrigo, R., 2008. The dendrochronology of *Callitris intratropica* in northern Australia: annual ring structure, chronology development and climate correlations. *Australian Journal of Botany* 56, 311–320.
- Bernard, F.R., 1983. Catalogue of the living Bivalvia of the eastern Pacific Ocean: Bering Strait to Cape Horn. Canadian Special Publication of Fisheries and Aquatic Sciences.
- Biondi, F., Cayan, D.R., Berger, W.H., 1999. Decadal-scale changes in southern California tree-ring records. In: Karl, T.R. (Ed.), *Proceedings of the 10th Symposium on Global Climate Change Studies*. American Meteorological Society, Boston, MA, pp. 303–306.
- Biondi, F., Gershunov, A., Cayan, D.R., 2001. North Pacific decadal climate variability since 1661. *Journal of Climate* 14, 5–10.
- Black, B.A., 2009. Climate driven synchrony across tree, bivalve, and rockfish growth-increment chronologies of the northeast Pacific. *Marine Ecology. Progress Series* 378, 37–46.
- Black, B.A., Boehlert, G.W., Yoklavich, M.M., 2008a. A tree-ring approach to establishing climate-growth relationships for yelloweye rockfish in the northeast Pacific. *Fisheries Oceanography* 5, 368–379.
- Black, B.A., Gillespie, D., MacLellan, S.E., Hand, C.M., 2008b. Establishing highly accurate production-age data using the tree-ring technique of crossdating: a case study for Pacific geoduck (*Panopea abrupta*). *Canadian Journal of Fisheries and Aquatic Sciences*.
- Bortolot, Z.J., Copenheaver, C.A., Longe, R.L., Van Aardt, J.A.N., 2001. Development of a white oak chronology using live trees and a post-Civil War cabin in south-central Virginia. *Tree-ring Research* 57, 197–203.
- Briffa, K.R., Osborn, T.J., Schweingruber, F.H., 2004. Large-scale temperature inferences from tree rings: a review. *Global and Planetary Change* 40, 11–26.
- Buntgen, U., Frank, D.C., Nievergelt, D., Esper, J., 2006. Summer temperature variations in the European Alps, AD 755–2004. *Journal of Climate* 19, 5606–5623.
- Cerrato, R.M., 2000. What fish biologists should know about bivalve shells. *Fisheries Research* 46, 39–49.
- Chowdhury, M.Q., et al., 2008. Nature and periodicity of growth rings in two Bangladeshi mangrove species. *IAWA Journal* 29, 265–276.
- Coan, E.V., Scott, P.V., Bernard, F.R., 2000. Bivalve seashells of western North America. Santa Barbara Museum of Natural History, Santa Barbara, CA.
- Cook, E.R., 1985. A time-series analysis approach to tree-ring standardization. University of Arizona, Tucson, AZ.
- Cook, E.R., Briffa, K.R., Meko, D.M., Graybill, D.A., Funkhouser, G., 1995. The segment length curse in long tree-ring chronology development for paleoclimatic studies. *Holocene* 5, 229–237.
- Cook, E.R., D'Arrigo, R.D., Mann, M.E., 2002. A well-verified, multiproxy reconstruction of the winter North Atlantic Oscillation index since AD 1400. *Journal of Climate* 15, 1754–1764.
- Cook, E.R., Woodhouse, C.A., Eakin, C.M., Meko, D.M., Stahle, D.W., 2004. Long-term aridity changes in the western United States. *Science* 306, 1015–1018.
- D'Arrigo, R., Wiles, G., Jacoby, G., Villalba, R., 1999. North Pacific sea surface temperatures: past variations inferred from tree rings. *Geophysical Research Letters* 26, 2757–2760.
- D'Arrigo, R., Mashig, E., Frank, D., Wilson, R., Jacoby, G., 2005a. Temperature variability over the past millennium inferred from Northwestern Alaska tree rings. *Climate Dynamics* 24, 227–236.
- D'Arrigo, R., et al., 2005b. Tropical-North Pacific climate linkages over the past four centuries. *Journal of Climate* 18, 5253–5265.
- D'Arrigo, R., Wilson, R., Jacoby, G., 2006a. On the long-term context for late twentieth century warming. *Journal of Geophysical Research-Atmospheres* 111.
- D'Arrigo, R., et al., 2006b. Monsoon drought over Java, Indonesia, during the past two centuries. *Geophysical Research Letters* 33.
- Esper, J., Cook, E.R., Schweingruber, F.H., 2002. Low-frequency signals in long tree-ring chronologies for reconstructing past temperature variability. *Science* 295, 2250–2253.
- Esper, J., Frank, D.C., Wilson, R.J.S., Briffa, K.R., 2005. Effect of scaling and regression on reconstructed temperature amplitude for the past millennium. *Geophysical Research Letters* 32.
- Fritts, H.C., 1976. *Tree Rings and Climate*. Academic Press, New York, 567 pp.
- Gedalof, Z., Smith, D.J., 2001. Dendroclimatic response of mountain hemlock (*Tsuga mertensiana*) in Pacific North America. *Canadian Journal of Forest Research* 31, 322–332.
- Gedalof, Z., Mantua, N.J., Peterson, D.L., 2002. A multi-century perspective of variability in the Pacific Decadal Oscillation: new insights from tree rings and coral. *Geophysical Research Letters* 29, 2204.
- Goodkin, N.F., Hughen, K.A., Cohen, A.L., Smith, S.R., 2005. Record of Little Ice Age sea surface temperatures at Bermuda using a growth-dependent calibration of coral Sr/Ca. *Paleoceanography* 20, 1–9.
- Grissino-Mayer, H.D., 2001. Evaluating crossdating accuracy: a manual and tutorial for the computer program COFECHA. *Tree-Ring Research* 57, 205–221.
- Guyette, R.P., Rabeni, C.F., 1995. Climate response among growth increments of fish and trees. *Oecologia* 104, 272–279.
- Halfar, J., et al., 2007. Coralline alga reveals first marine record of subarctic North Pacific climate change. *Geophysical Research Letters* 34, L07702.
- Helama, S., Schöne, B.R., Black, B.A., Dunca, E., 2006a. Constructing long-term proxy series for aquatic environments with absolute dating control using a sclerochronological approach: introduction and advanced applications. *Marine and Freshwater Research* 57, 591–599.
- Helama, S., Schöne, B.R., Black, B.A., Dunca, E., 2006b. Constructing long-term proxy series for aquatic environments with absolute dating control using a sclerochronological approach: introduction and advanced applications. *Marine and Freshwater Research* 57, 591–599.
- Helama, S., et al., 2007. Compound response of marine and terrestrial ecosystems to varying climate: pre-anthropogenic perspective from bivalve shell growth increments and tree-rings. *Marine Environmental Research* 63, 185–199.
- Hendy, E.J., Gagan, M.K., Lough, J.M., 2003. Chronological control of coral records using luminescent lines and evidence for non-stationary ENSO teleconnections in northeast Australia. *Holocene* 13, 187–199.
- Holmes, R.L., 1983. Computer-assisted quality control in tree-ring dating and measurement. *Tree-Ring Bulletin* 43, 69–78.
- IPCC, 2007. Working Group I Report “The Physical Science Basis”. Intergovernmental Panel on Climate Change.
- Kadonaga, L.K., Podlaha, O., Whitticar, M.J., 1999. Time series analyses of tree ring chronologies from Pacific North America: evidence for sub-century climate oscillations. *Chemical Geology* 161, 339–363.
- Lafon, C.W., Speer, J.H., 2002. Using dendrochronology to identify major ice storm events in oak forests of southwestern Virginia. *Climate Research* 20, 41–54.
- LeBreton, G.T.O., Beamish, F.W.H., 2000. Interannual growth variation in fish and tree rings. *Canadian Journal of Fisheries and Aquatic Sciences* 57, 2345–2356.
- MacDonald, G.M., Case, R.A., 2005. Variations in Pacific Decadal Oscillation over the past millennium. *Geophysical Research Letters* 32, L08703.
- Mann, M.E., Bradley, R.S., Hughes, M.K., 1998. Global-scale temperature patterns and climate forcing over the past six centuries. *Nature* 392, 779–787.
- Mantua, N.J., Hare, S.R., Zhang, Y., Wallace, J.M., Francis, R.C., 1997. A Pacific interdecadal climate oscillation with impacts on salmon production. *Bulletin of the American Meteorological Society* 78, 1069–1079.
- Moberg, A., Sonechkin, D.M., Imgren, K.H., Datsenko, N.M., Karién, W., 2005. Highly variable Northern Hemisphere temperatures reconstructed from low- and high-resolution proxy data. *Nature* 433, 613–617.
- Noakes, D.J., Campbell, A., 1992. Use of geoduck clams to indicate changes in the marine environment of Ladysmith Harbor, British Columbia. *EnvironMetrics* 3, 81–97.
- Pauling, A., Luterbacher, J., Wanner, H., 2003. Evaluation of proxies for European and North Atlantic temperature field reconstructions. *Geophysical Research Letters* 30.
- Peterson, D.W., Peterson, D.L., Ettl, G.J., 2002. Growth responses of subalpine fir to climatic variability in the Pacific Northwest. *Canadian Journal of Forest Research* 32, 1503–1517.
- Prieto, M.D., Herrera, R., Dussel, P., 1999. Historical evidences of streamflow fluctuations in the Mendoza River, Argentina, and their relationship with ENSO. *Holocene* 9, 473–481.
- Schöne, B.R., et al., 2003. North Atlantic Oscillation dynamics recorded in shells of a long-lived bivalve mollusk. *Geology* 31, 1037–1040.
- Schöne, B.R., Dunca, E., Mutvei, H., Norlund, U., 2004. A 217-year record of summer air temperature reconstructed from freshwater pearl mussels (*M. margaritifera*, Sweden). *Quaternary Science Reviews* 23, 1803–1816.
- Solomina, O., Davi, N., D'Arrigo, R., Jacoby, G., 2005. Tree-ring reconstruction of Crimean drought and lake chronology correction. *Geophysical Research Letters* 32.
- Stokes, M.A., Smiley, T.L., 1996. *An introduction to tree-ring dating*. The University of Arizona Press, Tucson, Arizona, 73 pp.
- Strom, A., 2003. *Climate and fisheries in the Pacific Northwest: historical perspectives from geoducks and early explorers*. Thesis (M.S.), University of Washington, 55pp.
- Strom, A., Francis, R.C., Mantua, N.J., Miles, E.L., Peterson, D.L., 2004. North Pacific climate recorded in growth rings of geoduck clams: a new tool for paleoenvironmental reconstruction. *Geophysical Research Letters* 31, L06206.
- Thompson, D.W.J., Kennedy, J.J., Wallace, J.M., Jones, P.D., 2008. A large discontinuity in the mid-twentieth century in observed global-mean surface temperature. *Nature* 453, 646–650.
- Thresher, R.E., Koslow, J.A., Morison, A.K., Smith, D.C., 2007. Depth-mediated reversal of the effects of climate change on long-term growth rates of exploited marine fish. *Proceedings of the National Academy of Sciences of the United States of America* 104, 7461–7465.
- Tompkins, J.D., Lamoureux, S.F., Sauchyn, D.J., 2008. Reconstruction of climate and glacial history based on a comparison of varve and tree-ring records from Mirror Lake, Northwest Territories, Canada. *Quaternary Science Reviews* 27, 1426–1441.
- Wigley, T.M.L., Briffa, K.R., Jones, P.D., 1984. On the average value of correlated time-series, with applications in dendroclimatology and hydrometeorology. *Journal of Climate and Applied Meteorology* 23, 201–213.
- Wiles, G.C., D'Arrigo, R.D., Jacoby, G.C., 1998. Gulf of Alaska atmosphere-ocean variability over recent centuries inferred from coastal tree-ring records. *Climatic Change* 38, 289–306.
- Wilson, R.J.S., Esper, J., Luckman, B.H., 2004. Utilising historical tree-ring data for dendroclimatology: a case study from the Bavarian Forest, Germany. *Dendrochronologia* 21, 53–68.
- Wilson, R.J.S., Luckman, B.H., Esper, J., 2005. A 500 year dendroclimatic reconstruction of spring-summer precipitation from the lower Bavarian Forest region, Germany. *International Journal of Climatology* 25, 611–630.
- Woodhouse, C.A., 2003. A 431-yr reconstruction of western Colorado snowpack from tree rings. *Journal of Climate* 16, 1551–1561.
- Yamaguchi, D.K., 1991. A simple method for cross-dating increment cores from living trees. *Canadian Journal of Forest Research* 21, 414–416.
- Yang, B., Bräuning, A., Zhang, Z., Dong, Z., Esper, J., 2007. Dust storm frequency and its relation to climate changes in Northern China during the past 1000 years. *Atmospheric Environment* 41, 9288–9299.